MICROCOPY RESOLUTION TEST CHART

DEPARTMENT OF DEFENCE

DEFENCE SCIENCE AND TECHNOLOGY ORGANISATION

MATERIALS RESEARCH LABORATORIES

MELBOURNE, VICTORIA

REPORT

MRL-R-976

RAIL INDUCTANCE CALCULATIONS FOR SOME
SIMPLE CURRENT DISTRIBUTIONS

V. Kowalenko

86   5   21   028

FEBRUARY, 1986

DEPARTMENT OF DEFENCE

MATERIALS RESEARCH LABORATORIES

REPORT

MRL-R-976

RAIL INDUCTANCE CALCULATIONS FOR SOME

SIMPLE CURRENT DISTRIBUTIONS

V. Kowalenko

ABSTRACT

In this study, an expression for the inductance per unit length of
the rails for a railgun-type electromagnetic launcher (EML) is derived from
first principles using simple quasi-stationary models for the current
distribution in the rails. The results are applied, in particular, to the
MRL railgun and are compared with work by others in the field. The study
concludes with discussions on the problems associated with current diffusion
in the rails, and the resulting influence upon the equation-of-motion used in
evaluating projectile performance.

Approved for Public Release

DOCUMENT CONTROL DATA SHEET

REPORT NO.	AR NO.	REPORT SECURITY CLASSIFICATION
MRL-R-976	AR-004-342	Unclassified

TITLE

Rail inductance calculations for some
simple current distributions

AUTHOR(S)	CORPORATE AUTHOR
V. Kowalenko	Materials Research Laboratories P.O. Box 50, Ascot Vale, Victoria 3032

REPORT DATE	TASK NO.	SPONSOR
FEBRUARY 1986	DST 82/212	DSTO

FILE NO.	REFERENCES	PAGES
G6/4/8 - 3020	14	43

CLASSIFICATION/LIMITATION REVIEW DATE	CLASSIFICATION/RELEASE AUTHORITY
	Superintendent, MRL Physics Division

SECONDARY DISTRIBUTION

Approved for Public Release

ANNOUNCEMENT

Announcement of this report is unlimited.

.EYWORDS

Electric guns, Railgun accelerators,	Electromagnetic launchers Current distribution Equations of motion Inductance

COSATI GROUPS	2103	1906

ABSTRACT

In this study, an expression for the inductance per unit length of
the rails for a railgun-type electromagnetic launcher (EML) is derived from
first principles using simple quasi-stationary models for the current
distribution in the rails. The results are applied, in particular, to the
MRL railgun and are compared with work by others in the field. The study
concludes with discussions on the problems associated with current diffusion
in the rails, and the resulting influence upon the equation-of-motion used in
evaluating projectile performance.

CONTENTS

A_p cross-sectional area of the bore, m^2

a length or width of each element in the grid in figure 5, m

$\underset{\sim}{B}$ magnetic field of induction, T

$\underset{\sim}{B}_z$ z-component of the magnetic field of induction, T

C capacitance of the capacitor bank of an electromagnetic launcher, F

d separation of the rails, m

$d\underset{\sim}{\ell}$ differential vector length element

$E(0)$ total initial energy stored by the capacitor bank, J

E_1 kinetic energy of the projectile, J

E_2 kinetic energy of the plasma armature, J

E_3 retarding energy term due to the gas ahead of the projectile, J

E_4 work done on overcoming the frictional forces on the projectile, J

E_5 work done on overcoming the frictional drag on the plasma armature, J

$F(t)$ accelerating force on the arc-projectile system, N

$f(t)$ general term involving drag and frictional forces on the arc-projectile system, N

$f_a(t)$ frictional drag on the plasma armature, N

$f_p(t)$ frictional force on the projectile, N

$H(t-t_s)$ Heaviside step-function

h height of the rails, m

h_A height of the plasma armature, m

$I(t)$ current in the railgun circuit at time t, A

I_{ij} current belonging to each element in the grid in figure 5, A

I_{max} maximum or peak current attained in a railgun firing, A

$\underset{\sim}{j}$	current density, A/m^2
L	total inductance due to both rails, H
ℓ	displacement of the projectile, m
L_o	inductance of the storage inductor, H
L'	rail inductance per unit length due to both rails, H/m
L_{int}	internal inductance of the rails, H/m
m	number of elements in a row in the grid in figure 5
m_a	mass of the plasma armature, kg
m_i	mass of ions belonging to species i in the plasma armature, kg
m_p	mass of the projectile, kg
N_i	number of ions belonging to species i in the plasma armature
n	number of elements in half of the column in the grid in Figure 5.
$P_s(t)$	shock pressure, Pa
Q	instantaneous charge stored by the capacitor bank, C
$R(t)$	total resistance in the railgun circuit, Ω
$\underset{\sim}{r}$	position vector
r	magnitude of position vector, m
$R'(t)$	effective time-dependent resistance per unit length of the rails, Ω/m
t	time measured from shot-start, s
$V_o(t)$	time-varying extraneous potential in railgun circuit, V
v	velocity of the arc-projectile system, m/s
v_i	average velocity of species i comprising the plasma armature
w	width of the rails, m
x	cartesian co-ordinate shown in Figure 1
y	cartesian co-ordinate shown in Figure 1

z	cartesian co-ordinate shown in Figure 1
$\delta(t)$	skin-depth or penetration depth at time t, m
$\overline{\delta}$	effective skin-depth as shown in Figure 1, m
μ	magnetic permeability, H/m
μ_o	magnetic permeability of the vacuum, H/m
σ	electrical conductivity of the rails, $(\Omega m)^{-1}$
Φ	total magnetic flux contribution due to both rails, Wb
Φ_ℓ	total magnetic flux contribution due to the left rail, Wb

RAIL INDUCTANCE CALCULATIONS FOR SOME

SIMPLE CURRENT DISTRIBUTIONS

1. INTRODUCTION

Electromagnetic launchers such as railguns are seen as an
alternative means of accelerating projectiles to significantly higher speeds
than conventional guns.   The projectiles in railguns are accelerated by means
of the interaction of an electric current with a magnetic field.   Exit
velocities up to 10 km/s have been measured [1] for small projectiles, and
higher velocities seem possible.   This high-velocity potential of railguns
makes them attractive in such defence applications as anti-ship missile
defence and anti-armour weapons.

One experimental railgun used at MRL consists basically of an
electric power supply connected to two long parallel conductors (the rails)
held within a transparent polycarbonate body.   The projectile is initially
placed near the open-breech end.   Current flows through a circuit consisting
of the rails driven from the power source, which consists typically of a
capacitor bank (C = 1.59 x 10^{-3} F) connected to a storage inductor
(L_o = 5.97 μH) by a switch.   A plasma-armature, produced initially by the
vapourisation of a small piece of metallic foil immediately behind the
projectile, serves as a conducting medium for the current to pass between the
rails.   The projectile is subsequently accelerated by the Lorentz ($j \times B$)
force produced by the interaction of the current in the plasma armature and
the magnetic field associated with the total current in the railgun system.
For a firing with the capacitor bank charged up to 6 kV and rails 0.5 m in
length the time taken for a projectile weighing 0.38 g and moving through a
bore cross-section of 0.48 cm^2 to exit is approximately 1 ms [2].

From an electrical point of view the railgun can be represented as a
lumped parameter circuit, in which various components of the system such as
the power source, the rails and plasma-armature are represented by constant or
time-varying capacitances, inductances and resistances.   In addition, a time-
varying current I(t) passes through the circuit.

1

If the effects of friction on the arc-projectile system are neglected, and assuming that no arcing occurs ahead of the projectile, the accelerating force F(t) on the arc-projectile system is given by

$$F(t) = \frac{1}{2} L' I(t)^2 \tag{1}$$

where L', which is normally assumed to be constant, represents the rail inductance per unit length. This rail inductance parameter clearly represents a vital physical quantity in describing the motion of the projectile in a railgun. A full derivation of equation (1) is given in Appendix A.

In this study, an expression for the inductance of the rails is derived analytically assuming that at any particular instant the current distribution in the rails can be represented by a constant current density extending from the inner rail boundary out to some effective skin, or penetration, depth $\overline{\delta}$. Further, it is considered that this distribution is the same for all positions along the rail up to the projectile position. It is expected that in general $\overline{\delta}$ will vary with the position of the projectile and its time-history in reaching that point. The resulting expression is then used to determine both a maximum and minimum value for the rail inductance, the maximum occurring when the current is confined to the inner rail (i.e. $\overline{\delta} \approx 0$) and the minimum occurring when the current is uniformly distributed throughout the rail cross-section (i.e. $\overline{\delta} = w$). Apart from these two limiting conditions, the method discussed here is of little use in analysing railgun performance because, in general, the values to be given to $\overline{\delta}$ can only be determined from a vigorous analysis of the problem.

The contents of the report are arranged as follows. In section 2 the model which is used to derive the rail inductance per unit length is presented and its assumptions are discussed. The magnetic field of induction between the rails is then obtained in integral form in section 3 using this model. The results of section 3 are used in section 4 to evaluate the rail inductance per unit length in the zero skin-depth limit. In section 5 the rail inductance per unit length is derived using a finite effective skin-depth along the rails. The resulting expression for the rail inductance per unit length is then modified for application to the Kerrisk CINDA current diffusion program [3] in section 6. In section 7 an additional term appearing in the equation of motion for the arc-projectile system due to the time-dependence of the rail inductance is examined and shown to be small for the railgun configuration used at MRL. In the concluding section 8, the problem of current diffusion into the rails is discussed.

2. DISCUSSION OF MODEL

An expression for the rail inductance can only be found if the current distribution within the rails is known. The current distribution can in principle be determined from the current diffusion, or penetration,

2

equation which is formulated from Maxwell's equations. The equation is a second-order partial-differential equation in three dimensions and is particularly difficult to solve. In addition the boundary conditions which are necessary for the solution of the equations are not adequately known for the railgun situation.

In general the penetration depth of current within a conductor is dependent upon the magnitude of the length parameter known as skin-depth. For instance, in cases where the current is initially confined to the inner surface of a conductor the subsequent current density is found to have an exponential dependence of $e^{-x/\delta}$ [4] where x is the penetration depth, and the skin-depth δ is given by:

$$\delta(t) = \left(\frac{t}{\pi\sigma\mu}\right)^{1/2} \tag{2}$$

Here σ represents the conductivity of the medium, μ is the magnetic permeability and t is the time. If the current density within the railgun conductor has the exponential dependence as shown above, then most of the current can be thought of as lying within one or two skin-depths of the surface.

The model used in this study considers that the current in both rails distributes itself uniformly and instantaneously from each of the inner surfaces of the rails to an effective skin-depth δ as indicated in figure 1. This effective skin-depth δ varies with time as will be discussed later. In figure 1 the rails are pictured as having a height h, width w and separation d. Current flows a distance ℓ along the left rail, passes through the plasma-armature and returns along the other rail. The height of the armature, h_A, is taken to be identical with the barrel-bore height which may not always be the case in practice.

It must be emphasised that the actual distribution of the current over the rail cross-section is far more complicated than this quasi-stationary model suggests. The longer the current passes a position along the rails the more it diffuses through the rail cross-section. Thus the current distribution in the rails is expected to be different everywhere along the rails but at the same time the total current must be conserved over the entire rail cross-section at each position along the rails. The main purpose in proposing this model is to derive an analytic expression for the rail inductance per unit length, which can then be incorporated into railgun simulation codes. The advantage in using this model is that by specifying increasing values for $\bar{\delta}$ as a function of time, allowance is made for the fact that the current is continually diffusing into the rails during the course of a firing. As will be shown later, previous analytic attempts have neglected the effect of current diffusion and this could have a substantial effect on the values of the rail inductance per unit length. From equation (1), any substantial effect on L' means an effect on the performance of a railgun.

The model proposed here means that the current changes abruptly at the boundaries between the rails and the plasma-armature. Any effect that such discontinuities may have on the rail inductance calculation is

neglected. It is further assumed that the contribution to the inter-rail
magnetic flux due to currents in the power sources leading to the breech of
the railgun is negligible.

Because the height of the plasma-armature, h_A, is much less than the
height of the rails for the MRL railgun and since the current must be
conducted through the armature, it follows that in the vicinity of the
armature nearly all of the current must be confined to the inner surfaces of
the rails. Further away from the plasma armature the current will also have
a tendency to remain close to the inner surface of the rails because of the
relatively slow diffusion rates obtained and because of the proximity effect
[5]. When this effect exists, currents flowing in opposite directions move
towards the inner surfaces of rectangular conductors with most of the current
in the corners. This behaviour has also been predicted by the numerical
calculations of Kerrisk [6], who has considered the high-frequency- limit
condition in order to calculate the current distribution in the rails and
hence the rail inductance. His method is essentially equivalent to evaluating
charge distribution on equipotential surfaces and neglects the fact that the
current, and hence both the magnetic and electric fields, are time-varying
throughout the duration of a firing.

The model for the current distribution in the rails used by
Hawke et al [7] and also by Sadedin [8], considers that at any point the
current density is constant from the inner surface of the rail out to an
effective penetration or skin depth δ based on equation (2). In this model
the value of δ varies with position along the rail being smallest immediately
behind the projectile but increasing with distance from the projectile because
the current has existed there longer than at points closer to the plasma
armature. This is therefore rather different to the Kerrisk model, which has
the same current distribution at each point along the rails. Even though the
Hawke model represents a simple model for the current distribution within the
rails it is nonetheless difficult to implement in rail inductance
calculations. (For further discussion of this model, the reader is referred
to Appendix B.) Therefore, the concept of an effective skin-depth given
by $\overline{\delta}$ has been introduced in this study.

It must be mentioned that the effective skin-depth model can be used
to replace more complicated current distributions. For instance it will be
shown later that the values for the rail inductance obtained numerically by
Kerrisk, who has considered a more complex current distribution assuming the
high-frequency limit, can be obtained using the effective skin-depth model.
Therefore, this model represents an equivalent but even simpler approach to
the rather complicated problem of current diffusion in the rails.

The effective skin-depth approach is seen as a further improvement
upon the current-sheet approach used by Thio [9] and Batteh [10]. In these
models the current is assumed to lie in the form of infinitesimally thin
sheets on the inner surfaces of the rails. The value for the rail inductance
per unit length obtained using this model is considered to be high compared
with values inferred from experimental studies. This offers a further
indication that the current distribution deviates quite markedly from the
current-sheet model. By introducing an effective skin-depth into rail
inductance calculations and then specifying values obtained from magnetic flux

4

measurements for this $\overline{\delta}$ an allowance for current diffusion into the rails is made and lower L'-values will be obtained.

It is interesting to note that the expression for the rail inductance per unit length derived in this study will yield both a maximum and minimum value. The maximum value for the rail inductance is found by considering the zero skin-depth limit or the limit as δ tends to zero. This is of course the current-sheet approach and in this limit agreement is found with the expression obtained by Thio [9]. On the other hand, the expression for the effective inductance given by Batteh [10] is slightly different even though he too uses the current-sheet model. The difference arises from the fact that Batteh has calculated the total $j \times B$ force of the armature and this introduces a dependence on the height of the armature, h_A, in his result. Agreement between Batteh's result and the expression derived in this report (equation (15)) is obtained in the limit where the armature height, h_A, is much less than the rail height, h, i.e. $h_A \ll h$.

The minimum value for the rail inductance is obtained when the current is uniformly distributed over the entire rail cross-section. This is in fact the large-time limit which is probably never attained in a railgun firing. To obtain an estimate of this time, equation (2) can be used. If the skin-depth is indeed given by this equation, then the time taken for the skin-depth to reach a value equivalent to the width of the rails for the MRL railgun, i.e. 12.5 mm, is approximately 0.025 s. Thus at each position along the rails where the current has had the opportunity to diffuse for a much longer time than 0.025 s., the current distribution will tend to become uniform over the entire rail cross-section. In view of the fact that a typical firing takes 1 ms., this situation is probably never attained at any point along the barrel unless of course equation (2) is not valid. Though the current does not become uniform over the entire rail cross-section at any point along the barrel the large time limit is nevertheless important. This is because in this limit the magnetic flux between the rails, and hence the rail inductance, becomes a minimum. Thus in this study the value for the rail inductance per unit length will be bounded above by the value obtained from the current-sheet model and below by the value obtained using the large-time limit.

It must also be mentioned that the material presented in this report can be used to calculate the $j \times B$ force of the armature. This can be done by using the magnetic field derived in section 3 along with the assumption that the current density within the armature is uniform. The latter assumption can be justified on the basis of experimental magnetic flux measurements [11]. The only problem such a calculation would present is that the magnetic field contribution near the plasma-armature, which now dominates this calculation, may be completely different from the magnetic field obtained using the models presented in this study.

5

3.   EVALUATION OF THE MAGNETIC INDUCTION BETWEEN THE RAILS

In this calculation the inductance of the rails is derived by the method of flux linkages.   This means that the total magnetic flux between the rails is calculated in the central plane where the point P (which has co-ordinates (x',y',0)) is situated as shown in figure 1.   The x, y and z axes are also indicated in this figure.

Although the magnetic flux contribution due to the current passing through the plasma-armature can be calculated [12] by assuming that the current density in the plasma-armature is uniform, it is negligible in comparison with the magnetic flux contribution due to the rails.   In addition, the internal rail inductance is neglected in this study but discussion of how it can be evaluated is left till after the magnetic field for the uniform effective skin-depth model is presented.   This latter assumption means in effect that the uncoupled flux in the railgun is considered negligibly small in comparison with the flux which occupies the space between the rails.

Because of symmetry, only the magnetic flux contribution due to one of the rails needs to be calculated.   This can then be doubled to obtain the total magnetic flux contribution due to both rails.   However, before the total magnetic flux can be determined, the magnetic field of induction, i.e. the magnetic flux density between the rails must be evaluated.   The magnetic field of induction due to a current in an element $d\underset{\sim}{\ell}$ situated at the position vector $\underset{\sim}{r}$ from the point of interest (the origin) is given by the Biot-Savart law as:

$$d\underset{\sim}{B} = \frac{\mu_o i}{4\pi} \frac{d\underset{\sim}{\ell} \times \underset{\sim}{r}}{r^3} \tag{3}$$

where r is the magnitude of the position vector $\underset{\sim}{r}$.   Therefore, using the assumption of uniform penetration of the current in the rails together with equation (3), the magnetic field of induction at the point P due to a current element of area dx dz and length dy in the left rail as shown in figure 1 is:

$$d\underset{\sim}{B} = \frac{\mu_o}{4\pi} \frac{I}{h\bar{\delta}} dz \, dx \frac{(dy \, \hat{y}) \times \left((x' - x)\hat{x} + (y' - y)\hat{y} - z\hat{z} \right)}{\left((x - x')^2 + (y - y')^2 + z^2 \right)^{3/2}} \tag{4}$$

where $0 < y' < \ell$ and $\bar{\delta} < x' < d + \bar{\delta}$.   Here, $\hat{x}$, $\hat{y}$ and $\hat{z}$ represent the unit vectors in the x, y and z directions respectively whilst $I/h\delta$ represents the uniform current density.

The z-component of the magnetic field of induction given in equation (4) is the component which contributes to the total magnetic flux.   This is because it is the only component not perpendicular to the surface vector in the z = 0 plane.   The z-component of the magnetic field of induction due to the left rail is:

6

$$dB_z = -\frac{\mu_o I}{4\pi h\bar{\delta}} \frac{dz\ dy\ dz\ (x' - x)}{\left((x - x')^2 + (y - y')^2 + z^2\right)^{3/2}} \hat{z} \tag{5}$$

The total B_z-contribution due to the left rail is found by integrating over all of the rail dimensions, giving:

$$B_z = \int_0^\ell \int_0^{\bar{\delta}} \int_{-h/2}^{h/2} \frac{\mu_o I}{4\pi h\bar{\delta}} \frac{(x - x')}{\left((x - x')^2 + (y - y')^2 + z^2\right)^{3/2}} \hat{z}\ dz\ dx\ dy \tag{6}$$

It is advisable to evaluate the dx-integral first because then the current sheet limit (the limit as $\delta \to 0$) can be considered immediately. Thus equation (6) becomes:

$$B_z = \int_0^\ell \int_{-h/2}^{h/2} \frac{\mu_o I}{4\pi h\bar{\delta}} \left(\frac{1}{\left((y'-y)^2 + x'^2 + z^2\right)^{1/2}} - \frac{1}{\left((y'-y)^2 + (x'-\bar{\delta})^2 + z^2\right)^{1/2}} \right) \hat{z}\ dz\ dy \tag{7}$$

4. ZERO SKIN-DEPTH CURRENT MODEL

In the important limit as $\bar{\delta} \to 0$, equation (7) reduces to:

$$B_z = -\int_0^\ell \int_{-h/2}^{h/2} \frac{\mu_o I}{4\pi h} \frac{x'}{\left((y'-y)^2 + x'^2 + z^2\right)^{3/2}} \hat{z}\ dz\ dy \tag{8}$$

The inductance of the rails will first be found using equation (8). The resulting expression for the rail inductance will then serve as a useful check when the rail inductance is found using equation (7) (the finite $\bar{\delta}$ case) later. After performing the double integration, equation (8) becomes:

$$B_z = |B_z| = \frac{\mu_o I}{2\pi h} \left(\text{artan}\left(\frac{h(\ell - y')}{2x'\left((\ell-y')^2 + x'^2 + h^2/4\right)^{1/2}} \right) + \text{artan}\left(\frac{hy'}{2x'\left(x'^2 + y'^2 + h^2/4\right)^{1/2}} \right) \right) \tag{9}$$

The above result represents the magnitude of the z-component of the magnetic field of induction at the point P as shown in figure 1 assuming that the current flows in the form of a thin sheet on the left rail. The magnitude of

the z-component of the magnetic field of induction at the point P due to the right rail is obtained by replacing each x' by d-x'.

The magnetic flux due to the left rail is now evaluated using equation (9) and becomes:

$$\phi_\ell = \int B_z \, dS = \int_o^\ell \int_o^d \frac{\mu_o I}{2\pi h} \left(\text{artan} \left(\frac{h(\ell - y')}{2x'\left[(\ell-y')^2 + x'^2 + h^2/4\right]^{1/2}} \right) \right.$$

$$\left. + \text{artan} \left(\frac{hy'}{2x'(x'^2 + y'^2 + h^2/4)^{1/2}} \right) \right) dx'dy' \qquad (10)$$

where the flux has been evaluated across the central plane where $0 < y' < \ell$ and $0 < x' < d$.

After performing the dy'-integration, equation (10) is written as:

$$\phi_\ell = \frac{\mu_o I}{\pi h} \int_o^d \left(\ell \, \text{artan} \left(\frac{h\ell}{2x' \, (\ell^2 + x'^2 + h^2/4)^{1/2}} \right) \right.$$

$$+ \frac{x'}{2} \ln \left| \frac{2(x'^2 + h^2/4)^{1/2} - h}{2(x'^2 + h^2/4)^{1/2} + h} \right|$$

$$\left. - \frac{x'}{2} \ln \left| \frac{2(\ell^2 + x'^2 + h^2/4)^{1/2} - h}{2(\ell^2 + x'^2 + h^2/4)^{1/2} + h} \right| \right) dx' \qquad (11)$$

The total magnetic flux due to both rails is obtained by evaluating the integral in equation (11) and multiplying the result by a factor of 2. By definition, the total magnetic flux is also equal to LI where L represents the inductance. Thus using this formula, the inductance of the rails is found to be

$$L = \frac{2\mu_o}{\pi h} \left(\ell d \, \text{artan} \left(\frac{h\ell}{2d(\ell^2+d^2+h^2/4)^{1/2}} \right) + \frac{\ell^2}{2} \left(\ln \left| \frac{(\ell^2+d^2+h^2/4)^{1/2} - h/2}{(\ell^2+d^2+h^2/4)^{1/2} + h/2} \right| - \right. \right.$$

$$\left. \ln \left| \frac{(\ell^2+h^2/4)^{1/2} - h/2}{(\ell^2+h^2/4)^{1/2} + h/2} \right| \right) + \frac{h\ell}{4} \left(\ln \left| \frac{(\ell^2+d^2+h^2/4)^{1/2} -\ell}{(\ell^2+d^2+h^2/4)^{1/2} +\ell} \right| - \ln \left| \frac{(\ell^2+h^2/4)^{1/2} -\ell}{(\ell^2+h^2/4)^{1/2} +\ell} \right| \right)$$

$$+ \frac{d^2}{2} \ln \left| \frac{(d^2+h^2/4)^{1/2} -h/2}{(d^2+h^2/4)^{1/2} +h/2} \right| - \frac{h}{2} \left(\frac{h^2}{4} + d^2 \right)^{1/2} + \frac{h^2}{4} + \frac{(\ell^2+d^2)}{2} \ln \left| \frac{(\ell^2+d^2+h^2/4)^{1/2} -h/2}{(\ell^2+d^2+h^2/4)^{1/2} +h/2} \right|$$

$$- \frac{\ell^2}{2} \ln \left| \frac{(\ell^2 + h^2/4)^{1/2} - h/2}{(\ell^2 + h^2/4)^{1/2} + h/2} \right| - \frac{h}{4} \left(\frac{h^2}{4} + d^2 + \ell^2 \right)^{1/2} + \frac{h}{4} \left(\frac{h^2}{4} + \ell^2 \right)^{1/2} \right) \tag{12}$$

Equation (12) is a general result for the rail inductance. The rail inductance per unit length, i.e. L', is obtained by taking the derivative of equation (12) with respect to ℓ. Since equation (12) is rather complex, a more convenient but still useful L' is found by considering the large ℓ-limit. The large ℓ-limit, the meaning of which is discussed later, entails only evaluating the artan-integral in equation (11). In this limit the rail inductance becomes:

$$L \sim \frac{2\mu_o}{\pi h} \left(\ell d \ \text{artan} \left(\frac{h\ell}{2d \ (\ell^2 + d^2 + h^2/4)^{1/2}} \right) + \frac{\ell^2}{2} \left(\ln \left| \frac{(\ell^2 + d^2 + h^2/4)^{1/2} - h/2}{(\ell^2 + d^2 + h^2/4)^{1/2} + h/2} \right| \right. \right.$$

$$\left. \left. - \ln \left| \frac{(\ell^2 + h^2/4)^{1/2} - h/2}{(\ell^2 + h^2/4)^{1/2} + h/2} \right| \right) + \frac{h\ell}{4} \left(\ln \left| \frac{(\ell^2 + d^2 + h^2/4)^{1/2} - \ell}{(\ell^2 + d^2 + h^2/4)^{1/2} + \ell} \right| - \ln \left| \frac{(\ell^2 + h^2/4)^{1/2} - \ell}{(\ell^2 + h^2/4)^{1/2} + \ell} \right| \right) \right) \tag{13}$$

or more approximately,

$$L \sim \frac{2\mu_o}{\pi h} \left(\ell d \ \text{artan} \left(\frac{h}{2d} \right) + \frac{h}{4} \ell \ \ln \left| 1 + \frac{4d^2}{h^2} \right| \right) \tag{14}$$

The rail inductance per unit length (L'= dL/dℓ) derived from equation (14) is:

$$L' \sim \frac{2\mu_o}{\pi h} \left(d \ \text{artan} \left(\frac{h}{2d} \right) + \frac{h}{4} \ln \left| 1 + \frac{4d^2}{h^2} \right| \right) \tag{15}$$

Equation (15) has been obtained by Thio [9], who has used a mid-point average technique of the magnetic field result for the current-sheet model given in reference [6]. Although expressed in a different co-ordinate system, the magnetic field result used by Thio is identical to equation (9) in this study. Thus it is not surprising that agreement exists between his result and equation (15).

Equation (15) has also been obtained by Batteh [10] provided the assumption is made that the armature height is considerably smaller than the rail height, i.e. h_A <<h. Because there is a dependence on armature height appearing in Batteh's expression for the effective inductance per unit length of the plasma armature, his calculation is rather different from the present calculations which are concerned only with the evaluation of the inductance per unit length of the rails. It is the rail inductance per unit length and not Batteh's effective inductance per unit length which appears in the equation-of-motion of the arc-projectile system in the railgun (see Appendix A). For the MRL railgun, where the d/h ratio is 0.65, equation (15) yields a value of 0.54 μH/m.

The large ℓ-limit is obtained by finding the value of ℓ at which the rail inductance as given by equation (12) divided by ℓ yields the rail inductance per unit length as given by equation (15). For the MRL railgun the value of ℓ at which L/ℓ approaches 0.54 µH/m is 5 cm. Therefore before the large ℓ-limit, and hence equation (15), is valid the projectile must have travelled at least 5 cm (approximately one tenth the length of the gun barrel). In the recent Rapid Plasma Intensity Profiles (RPIP) series of experiments conducted at MRL [13], the time taken for the projectile to move 5 cm was about 190 µs. Thus before the large ℓ-limit can be considered for the MRL railgun the railgun must already be in its inductively driven stage as opposed to the earlier capacitively driven stage.

A plot of the rail inductance per unit length as given by equation (15) against values of d/h is presented in Figure 2. The graph shows that by increasing the d/h-ratio (either by increasing the separation of the rails or decreasing the height of the rails), the rail inductance per unit length and hence the maximum accelerating force on the arc-projectile system (equation (1)) also increases. In addition the graph indicates that for values of d/h greater than 10 the increase in L' is only gradual due to the logarithmic nature of equation (15). Thus a separation-to-height ratio (d/h) of about 10 would seem to be a suitable design ratio for railguns although other factors such as plasma stability not considered in this study might require lower values of d/h.

A peak current of 82 kA was achieved during the RPIP series, from which it follows that the greatest possible force on the arc-projectile system, which is given by $L'I_{max}^2/2$, is approximately 1.8×10^3 N. A value of L' = 0.54 µH/m calculated from equation (15) has been used. This means that the maximum acceleration is 6.0×10^6 m/s^2 for a combined mass of 0.30 g for the arc and projectile. If such an acceleration applied over the duration of a firing it would mean the exit velocity would only be 2.4 km/s. Defining the efficiency as the ratio of the kinetic energy on exit to the initial input energy an exit velocity of 2.4 km/s would correspond to a maximum efficiency of about 3% for a 6kV firing using the MRL railgun (C = 1.59×10^{-3}F).

5. FINITE SKIN-DEPTH CURRENT MODEL

The z-component of the magnetic field of induction for the finite skin-depth case ($\delta > 0$) is given by equation (7). After performing the double integration, equation (7) becomes:

$$\underset{\sim}{B}_z = -\frac{\mu_o I}{2\pi h \bar{\delta}} \hat{z}((\ell - y') \ln \left| \frac{\frac{h}{2} + \left((\ell - y')^2 + (x' - \bar{\delta})^2 + h^2/4\right)^{1/2}}{\frac{h}{2} + \left((\ell - y')^2 + x'^2 + h^2/4\right)^{1/2}} \right|$$

$$+ y' \ln \left| \frac{\frac{h}{2} + \left(y'^2 + (x' - \bar{\delta})^2 + h^2/4\right)^{1/2}}{\frac{h}{2} + \left(x'^2 + y'^2 + h^2/4\right)^{1/2}} \right|$$

$$- \pi\bar{\delta} - x' \, \text{artan} \left(\frac{- 2x'^2 - h^2/2 - h \left(x'^2 + y'^2 + h^2/4\right)^{1/2}}{2x'y'} \right)$$

$$- x' \, \text{artan} \left(\frac{- 2x'^2 - h^2/2 - h \left((\ell - y')^2 + x'^2 + h^2/4\right)^{1/2}}{2x' (\ell - y')} \right)$$

$$+ (x' - \bar{\delta}) \, \text{artan} \left(\frac{- 2(x' - \bar{\delta})^2 - h^2/2 - h \left(y'^2 + (x' - \bar{\delta})^2 + h^2/4\right)^{1/2}}{2y' (x' - \bar{\delta})} \right)$$

$$+ (x' - \bar{\delta}) \, \text{artan} \left(\frac{- 2(x' - \bar{\delta})^2 - h^2/2 - h \left((\ell - y')^2 + (x' - \bar{\delta})^2 + h^2/4\right)^{1/2}}{2(x' - \bar{\delta}) (\ell - y')} \right)$$

$$+ \frac{h}{2} \ln \left| \frac{y' + \left(y'^2 + (x' - \bar{\delta})^2 + h^2/4\right)^{1/2}}{\left((x' - \bar{\delta})^2 + h^2/4\right)^{1/2}} \right|$$

$$+ \frac{h}{2} \ln \left| \frac{\ell - y' + \left((\ell - y')^2 + (x' - \bar{\delta})^2 + h^2/4\right)^{1/2}}{\left((x' - \bar{\delta})^2 + h^2/4\right)^{1/2}} \right|$$

$$- \frac{h}{2} \ln \left| \frac{y' + \left(y'^2 + x'^2 + h^2/4\right)^{1/2}}{\left(x'^2 + h^2/4\right)^{1/2}} \right|$$

$$- \frac{h}{2} \ln \left| \frac{\ell - y' + \left((\ell - y')^2 + x'^2 + h^2/4\right)^{1/2}}{\left(x'^2 + h^2/4\right)^{1/2}} \right|$$

$$+ \frac{(\ell - y')}{2} \ln \left| \frac{(\ell - y')^2 + x'^2}{(\ell - y')^2 + (x' - \bar{\delta})^2} \right| + \frac{y'}{2} \ln \left| \frac{x'^2 + y'^2}{y'^2 + (x' - \bar{\delta})^2} \right|$$

11

$$+ \ x' \ \text{artan} \ \left(\frac{\ell - y'}{x'}\right) + x' \ \text{artan} \ \left(\frac{y'}{x'}\right)$$

$$- \ (x' - \bar{\delta}) \ \text{artan} \ \left(\frac{\ell - y'}{x' - \bar{\delta}}\right) - (x' - \bar{\delta}) \ \text{artan} \ \left(\frac{y'}{x' - \bar{\delta}}\right)) \qquad (16)$$

Equation (16) is quite general in that it is valid for any point in the central plane. A comparison of equations (16) and (9) shows that the introduction of a finite skin-depth δ greatly complicates the expression for the magnetic field of induction between the rails. The $\bar{B}_z$-contribution due to the right rail is obtained by replacing each $(x' - \delta)$ by $(d + \delta - x')$.

In order to evaluate the internal inductance of the rails, equation (16) would have to be generalised to include any point P with co-ordinates (x',y',z') in the rails. After this is done the energy density must be found, which would require the square of the general magnetic field result. The total energy in the rails is obtained by integrating over the entire volume of the rails and this is then set equal to $\frac{1}{2} L_{int} I^2$, where L_{int} is the internal inductance of the rails. In this analysis internal inductances are neglected in comparison with the external inductance.

The magnetic flux contribution due to the left rail is found following the same approach used to derive the magnetic flux in the zero skin-depth limit (i.e. equation (10)). It is noted that the magnetic flux contribution within the left rail, i.e. for $0 < x' < \bar{\delta}$, is found to equal zero when the substitution of variable $t = \bar{\delta} - x'$ is made in each integral containing the variable $x' - \bar{\delta}$. Thus the magnetic flux due to the left rail for a finite δ becomes:

$$\Phi_\ell = \frac{\mu_o I}{2\pi h \bar{\delta}} \ \int_{\bar{\delta}}^{d+\bar{\delta}} \ (\ell^2 \ \ell n \ \left| \frac{h/2 + (\ell^2 + (x' - \bar{\delta})^2 + h^2/4)^{1/2}}{h/2 + (\ell^2 + x'^2 + h^2/4)^{1/2}} \right|$$

$$+ \frac{\ell^2}{2} \ \ell n \ \left| \frac{\ell^2 + x'^2}{\ell^2 + (x' - \bar{\delta})^2} \right|$$

$$+ 2(x' - \bar{\delta})\ell \ \text{artan} \ \left(\frac{(x' - \bar{\delta})\ell}{(x' - \bar{\delta})^2 + h^2/4 + \left(\ell^2 + (x' - \bar{\delta})^2 + h^2/4 \right)^{1/2} h/2} \right)$$

$$+ \frac{h}{2} \ \left((x' - \bar{\delta})^2 + h^2/4 \right)^{1/2} - \frac{h}{2} \ \left(x'^2 + h^2/4 \right)^{1/2}$$

$$- 2\ell x' \arctan \left(\frac{x'\ell}{x'^2 + h^2/4 + (\ell^2 + x'^2 + h^2/4)^{1/2} h/2}\right)$$

$$- \frac{h}{2} \left(\ell^2 + (x' - \bar{\delta})^2 + h^2/4\right)^{1/2} + \frac{h}{2} \left(\ell^2 + x'^2 + h^2/4\right)^{1/2}$$

$$+ 2x'\ell \arctan \left(\frac{\ell}{x'}\right) - 2(x' - \bar{\delta})\ell \arctan \left(\frac{\ell}{x' - \bar{\delta}}\right) - \frac{x'^2}{2} \ln \left|\frac{\ell^2 + x'^2}{x'^2}\right|$$

$$+ \frac{(x' - \bar{\delta})^2}{2} \ln \left|\frac{\ell^2 + (x' - \bar{\delta})^2}{(x' - \bar{\delta})^2}\right| + x'^2 \left|\frac{h/2 + (\ell^2 + x'^2 + h^2/4)^{1/2}}{h/2 + (x'^2 + h^2/4)^{1/2}}\right|$$

$$- (x' - \bar{\delta})^2 \ln \left|\frac{h/2 + (\ell^2 + (x' - \bar{\delta})^2 + h^2/4)^{1/2}}{h/2 + ((x' - \bar{\delta})^2 + h^2/4)^{1/2}}\right|$$

$$+ h\ell \ln\left|\frac{\ell + (\ell^2 + (x' - \bar{\delta})^2 + h^2/4)^{1/2}}{\ell + (\ell^2 + x'^2 + h^2/4)^{1/2}}\right| + \frac{h\ell}{2} \ln \left|\frac{x'^2 + h^2/4}{(x' - \bar{\delta})^2 + h^2/4}\right|\right) dx' \tag{17}$$

All of the integrals appearing in equation (17) can be evaluated after some manipulation. However, the resulting expression from equation (17) which will yield the inductance of the rails once it is multiplied by $(2/I)$ is a very much more complicated expression than its equivalent for the $\delta = 0$ case, i.e. equation (12). Once again a more useful rail inductance expression is found by considering the large ℓ-limit (i.e. $\ell > 5$ cm) for equation (17). In this limit equation (17) becomes:

$$\Phi_\ell \sim \frac{\mu_o I}{2\pi h \bar{\delta}} \int_{\bar{\delta}}^{d+\bar{\delta}} \left(2(x' - \bar{\delta})\ell \arctan \left(\frac{x' - \bar{\delta}}{h/2}\right) - 2x'\ell \arctan \left(\frac{x'}{h/2}\right)\right.$$

$$\left. + \pi\ell\bar{\delta} + \frac{h\ell}{2} \ln \left|\frac{x'^2 + h^2/4}{(x' - \bar{\delta})^2 + h^2/4}\right|\right) dx' \tag{18}$$

13

After evaluation of the integrals and multiplication of the resulting expression by 2/I, equation (18) yields the following expression for the inductance of the rails:

$$L \sim \frac{\mu_o \ell}{\pi h \bar{\delta}} \left(\left(h^2/4 - (d + \bar{\delta})^2 \right) \text{artan} \left(\frac{2(d + \bar{\delta})}{h} \right) - \left(h^2/4 - \bar{\delta}^2 \right) \text{artan} \left(\frac{2\bar{\delta}}{h} \right) \right.$$

$$- \left(h^2/4 - d^2 \right) \text{artan} \left(\frac{2d}{h} \right) + \frac{hd}{2} \ell n \left| \frac{(d + \bar{\delta})^2 + h^2/4}{d^2 + h^2/4} \right| + \pi d \bar{\delta}$$

$$\left. + \frac{h\bar{\delta}}{2} \ell n \left| \frac{(d + \bar{\delta})^2 + h^2/4}{\bar{\delta}^2 + h^2/4} \right| \right) \tag{19}$$

For small $\bar{\delta}$, i.e. $\bar{\delta}/h \ll 1$ and $\bar{\delta}/d \ll 1$, equation (19) becomes:

$$L \sim \frac{2\mu_o \ell}{\pi h} \left(d \, \text{artan} \left(\frac{h}{2d} \right) + \frac{h}{4} \ell n \left| 1 + \frac{4d^2}{h^2} \right| - \frac{\bar{\delta}}{2} \text{artan} \left(\frac{2d}{h} \right) \right) \tag{20}$$

In the limit as $\bar{\delta} \rightarrow 0$, equation (20) reduces to equation (14) as expected.

The rail inductance per unit length (L') is obtained by dividing equation (19) by ℓ. A plot of L' against δ is shown in figure 3. This graph shows that for a d/h ratio equal to 0.65 (the situation for the MRL railgun), L' decreases quite substantially as the effective skin-depth δ increases.

A minimum value for L' can be found if $\bar{\delta}$ is set equal to the width of the rails. In this, the large time-limit, the current has had enough time to distribute itself uniformly over the entire rail cross-section. The value of L' obtained by setting $\bar{\delta}$ equal to 12.5 mm with d/h still equal to 0.65 is approximately 0.32 µH/m. When this value is compared with 0.54 µH/m (the $\delta = 0$ result) it represents a 40% reduction in L' and hence, by equation (1), a 40% reduction in the maximum accelerating force on the projectile. Thus if a decrease in L' due to significant current diffusion into the rails were to occur, the performance of the railgun would be affected quite substantially. It is therefore desirable that the width of the rails in a railgun be kept to a minimum in order to restrain the current diffusion occurring in the rails.

For the case of square rails, and with $\bar{\delta} = w$, the rail inductance per unit length becomes:

$$L' \sim \frac{\mu_o}{\pi} \left(\left(-\frac{3}{4} - \frac{2d}{h} - \left(\frac{d}{h}\right)^2 \right) \text{artan}\left(2\left(\frac{d}{h} + 1\right)\right) + \frac{3}{4} \text{artan}(2) \right.$$

$$+ \left(\left(\frac{d}{h}\right)^2 - \frac{1}{4} \right) \text{artan}\left(\frac{2d}{h}\right) + \frac{d}{2h} \ell n \left| \frac{\left(\frac{d}{h}\right)^2 + 2\left(\frac{d}{h}\right) + \frac{5}{4}}{\left(\frac{d}{h}\right)^2 + 1} \right| + \pi\left(\frac{d}{h}\right)$$

$$\left. + \frac{1}{2} \ell n \left| \frac{\left(\frac{d}{h}\right)^2 + 2\left(\frac{d}{h}\right) + \frac{5}{4}}{\frac{5}{4}} \right| \right) \tag{21}$$

The graph of L' as given by the above equation against d/h is shown in figure 4. Once again the rail inductance per unit length increases with increasing d/h ratio. The graph also confirms the behaviour found previously in the $\bar{\delta} = 0$ limit, where for values of d/h greater than 10 the increase in L' is only gradual. Thus there is not much gain in constructing a railgun with a separation-to-width ratio greater than 10.

Since the effective skin-depth $\bar{\delta}$ is time-dependent, the rail inductance per unit length is also time-dependent. If the effective skin-depth for the MRL railgun experiments is given by equation (2), then L' can be bounded by its value at t $\simeq$ 190 µs (the time at which the large ℓ-limit becomes valid) and by its value at the time of projectile exit (t $\simeq$ 1.0 ms). For copper-cadmium rails the conductivity σ equals 4.0×10^7 $(\Omega m)^{-1}$. The skin-depth for t $\simeq$ 190 µs is about 1.0 mm while for t = 1.0 ms, δ is approximately equal to 2.5 mm. Thus, during the acceleration of the projectile in the inductively-driven stage the value of the rail inductance per unit length using equation (20) will vary between

$$0.51 \text{ µH/m} > L'(t) > 0.47 \text{ µH/m} \tag{22}$$

This simple model indicates that there is a considerable decrease in the maximum accelerating force (equation (1)) of about 13% at projectile exit when compared with the value for L' using equation (15).

The rail inductance per unit length has been calculated numerically by Kerrisk [4] in the high-frequency limit. In that study it is assumed that the current is distributed over the surfaces of the rails. For square rails, and a d/h ratio equal to 0.5, Kerrisk has obtained a value of 0.30 µH/m for L'. The rail inductance per unit length for the current sheet limit is obtained using equation (15) with d/h equal to 0.5 and yields a value of 0.45 µH/m. For the other extreme where the current is uniformly distributed over the entire square cross-section equation (21) with d/h equal to 0.5 yields a value of 0.18 µH/m for L'. Thus the value obtained by Kerrisk falls, as expected, in the range of the two limiting values for L'. An effective skin-depth to rail height ratio ($\bar{\delta}$/h) of about 0.49 will yield an equivalent L' value to that obtained by Kerrisk. For the MRL railgun (square rails with

15

d/h equal to 0.65) an approximate value for L' obtained by Kerrisk would be 0.34 µH/m, which corresponds to an effective skin-depth of about 10 mm.

It is also interesting to note that the value of 0.30 µH/m obtained by Kerrisk for d/h equal to 0.5 represents a 33% reduction compared with the value of the rail inductance per unit length obtained using the current sheet model. Thus even in the high-frequency limit the maximum accelerating force on the arc-projectile system is substantially reduced when compared with the force that can be obtained using the rather ideal current sheet model. This reinforces the desirability of using rails of minimal thickness.

6. APPLICATION TO THE KERRISK CURRENT-DIFFUSION MODEL

So far it has been shown that the rail inductance per unit length is dependent on the current distribution over the rail cross-section. This distribution is determined by the diffusion of current into the rails. The current diffusion is time-dependent and hence L' is also time-dependent.

Current distribution over the rail cross-section is much more complicated than the rather simple models proposed in the previous sections. Kerrisk has analysed the problem of current diffusion in the rails by using a finite-difference formulation to solve the appropriate electric field equation for the rails. In this section it will be shown how the solution of equation (18) can be applied to a finite difference scheme for a more complex current distribution and in so doing it will be shown how another analytical expression for the rail inductance per unit length will be derived. The resulting expression for the total magnetic flux contribution due to the left rail which is linked to L' by multiplying it by the factor of $2/(\ell I)$ will be much more complicated than the expressions obtained earlier. However, this expression will require the specification of the current distribution in the rail cross-section. The specification of the current distribution in the rail cross-section at various times during acceleration is not discussed in this study.

A finite-difference formulation of the current diffusion problem requires that the rail cross-section be described by various current elements in a grid or mesh as shown in figure 5. Each element in the figure has a current I_{ij} and the sum of all of these currents equals I the total current in the railgun circuit. Although not necessary, it will be assumed that each of the elements has the same cross-sectional area of a^2 for the purpose of simplicity. The height of the rails is set equal to 2na where n is an integer while the width is set equal to ma with m also an integer. In the figure n equals 4 and m equals 6. The rails are separated by a distance d as before.

By symmetry, the currents in the various elements distribute themselves as shown in figure 5. Here it can be seen that the current in an element in a column in the upper half of a rail is the same as that for the corresponding element in that column for the lower half of the plane.

The first column (I_{i1}) of current elements belonging to a rail cross-section will now be considered. In this column a current of I_{11} resides in the corners of the rails. A current of I_{21} resides in the elements immediately below and above those in the corners while a current of I_{31} resides in the elements immediately below and above those elements with the currents of I_{21}. This situation continues until the last current is I_{n1} which resides in the elements immediately above and below the half plane of the rail.

The situation just described can be interpreted in a different manner. One can say that a current of I_{11} resides over the entire height of the column, i.e. h, while a current of ($I_{21} - I_{11}$) resides over a height (h-2a) of the column. Hence a current of ($I_{31} - I_{21}$) resides over a height (h-4a) of the column. In general then, a current of ($I_{i1} - I_{i-11}$) with $I_{01} = 0$ resides over a height (h-2(i-1)a) of the column. The sum of all of these currents over the heights to which they are valid will produce the current distribution as shown in figure 5.

The total magnetic flux for the first column is found by summing the individual magnetic flux contributions for the currents $I_{i1} - I_{i-11}$ over their heights of h-2(i-1)a. Thus equation (19) can be used except that the current I and height h are replaced by $I_{i1} - I_{i-11}$ and h-2(i-1)a respectively.

The total magnetic flux for the first column of the left rail in the large ℓ-limit is therefore:

$$\Phi_\ell \sim \frac{\mu_o \ell}{2\pi a} \sum_{i=1}^{n} \frac{(I_{i1} - I_{i-11})}{(h-2(i-1)a)} \left(\left(\frac{(h-2(i-1)a)^2}{4} - (d+a)^2 \right) \times \right.$$

$$\text{artan}\left(\frac{2(d+a)}{h-2(i-1)a}\right) - \left(\frac{(h-2(i-1)a)^2}{4} - a^2\right) \text{artan}\left(\frac{2a}{h-2(i-1)a}\right) + \pi da$$

$$- \left(\frac{(h-2(i-1)a)^2}{4} - d^2\right) \text{artan}\left(\frac{2d}{h-2(i-1)a}\right) + \frac{(h-2(i-1)a)d}{2} \times$$

$$\ln \left| \frac{(d+a)^2 + \frac{(h-2(i-1)a)^2}{4}}{d^2 + \frac{(h-2(i-1)a)^2}{4}} \right|$$

$$+ \frac{(h-2(i-1)a)a}{2} \ln \left| \frac{(d+a)^2 + \frac{(h-2(i-1)a)^2}{4}}{a^2 + \frac{(h-2(i-1)a)^2}{4}} \right| \right)$$

(23)

Before the total magnetic flux due to the j-th column of elements can be evaluated, equation (18) requires modification. This modification is necessary because the aim throughout this study has been to evaluate the total magnetic flux between the inner surfaces of the rails. Thus for each column the limits of the integral will be different. If for the time being the j-th column is assumed to have a uniform distribution of current then equation (18) becomes:

$$\Phi_\ell \sim \frac{\mu_o I}{2\pi ah} \int_{ja}^{d+ja} \Big(2(x'-a)\, \ell \, \text{artan}\,(\frac{x'-a}{h/2}) - 2x'\ell \, \text{artan}\,(2x'/h)$$

$$+ \pi\ell a + \frac{h\ell}{2}\, \ell n\, \Big| \frac{x'^2 + h^2/4}{(x'-a)^2 + h^2/4} \Big| \Big)\; dx'$$

$$\sim \frac{\mu_o I\ell}{2\pi ah} \Big((h^2/4 - (d+ja)^2)\, \text{artan}\,(\frac{d+ja}{h/2}) + ((ja)^2 - h^2/4)\, \text{artan}\,(\frac{ja}{h/2})$$

$$+ \Big((d+(j-1)a)^2 - h^2/4 \Big)\, \text{artan}(\frac{d+(j-1)a}{h/2}) - \Big(((j-1)a)^2 - h^2/4 \Big)\, \text{artan}(\frac{(j-1)a}{h/2})$$

$$+ \pi da + \frac{h}{2}\, d\, \ell n\, \Big| \frac{(d+ja)^2 + h^2/4}{(d+(j-1)a)^2 + h^2/4} \Big| + \frac{h}{2}\, ja\, \ell n\, \Big| \frac{(d+ja)^2 + h^2/4}{(ja)^2 + h^2/4} \Big|$$

$$- \frac{h}{2}\, (j-1)a\, \ell n\, \Big| \frac{(d+(j-1)a)^2 + h^2/4}{((j-1)a)^2 + h^2/4} \Big| \Big) \tag{24}$$

Now the case where each of the elements in the j-th column has a different current can be considered. The same procedure to evaluate equation (23) can be adopted except that each I is replaced with $I_{ij} - I_{i-1j}$ and each h is replaced by h-2(i-1)a. In this case each I_{0j} will be zero.

The total magnetic flux due to the entire left rail is found by summing over all columns in the grid, which becomes:

$$\Phi \sim \frac{\mu_o \ell}{2\pi} \sum_{j=1}^{m} \sum_{i=1}^{n} \frac{(I_{ij} - I_{i-1j})}{2(n+1-i)} \Big((n+1-i)^2 - (\frac{d}{a} + j)^2 \Big)\, \text{artan}\,(\frac{d/a + j}{n+1-i})$$

$$+ (j^2 - (n+1-i)^2)\, \text{artan}\,(\frac{j}{n+1-i}) + \Big((d/a+j-1)^2 - (n+1-i)^2 \Big)\, \text{artan}(\frac{d/a+j-1}{n+1-i})$$

18

$$- \left((j-1)^2 - (n+1-i)^2 \right) \, \text{artan} \left(\frac{j-1}{n+1-i} \right) + \pi d/a$$

$$+ (n+1-i) \, \frac{d}{a} \, \ln \left| \frac{(d/a+j)^2 + (n+1-i)^2}{(d/a+j-1)^2 + (n+1-i)^2} \right| + (n+1-i)j \, \ln \left| \frac{(d/a+j)^2 + (n+1-i)^2}{j^2 + (n+1-i)^2} \right|$$

$$- (n+1-i)(j-1) \, \ln \left| \frac{(d/a + (j-1))^2 + (n+1-i)^2}{(j-1)^2 + (n+1-i)^2} \right|) \tag{25}$$

The inductance per unit length for both rails is obtained by multiplying equation (25) by a factor of 2 and then dividing by ℓI. As a matter of interest, for the rail inductance per unit length not to be time-dependent each of the currents in the elements of the grid I_{ij} must possess the same time-dependence as the total current I in the circuit, which equals $\sum_{j=1}^{m} \sum_{i=1}^{n} I_{ij}$. Whether this is so depends on the solution of the current diffusion equation.

The above analysis can be extended quite easily to the situation where the grid consists of rectangular elements rather than square elements. It could also be extended to the situation where the x-z current distribution is changing in the y- (length) direction. This is the situation where the current through 3-dimensional blocks would need to be considered. However before this situation can be considered some modification to the previous results is required. One would have to return to equation (6) and evaluate the dy-integral over the length of each block rather than the displacement of the projectile. The total B_z-contribution due to the left rail could then be found by summing over all of the blocks in the rail. The reader should take note that the dy'-integral in equation (10) remains unaffected and thus it may be possible to consider the large ℓ-limit.

It is anticipated that by running the Kerrisk current diffusion program, or any similar program, which will yield values for the various I_{ij}'s appearing in equation (25), a more realistic value of L' and its variation with time will be obtained.

7. TIME-DEPENDENCE OF RAIL INDUCTANCE

Many of the solutions of the current diffusion equation given in reference [4] possess a time-dependence that is a product of circuit current and the exponential dependence $e^{-x/\delta}$ where δ is given by equation (2). From this it can be inferred that each of the I_{ij}'s appearing in equation (25) will not only possess the same time dependence as railgun current (I) but also a time-dependence to account for diffusion. Hence L' will become a time-dependent quantity.

If L' does possess a time-dependence, then the accelerating force on the arc-projectile system (still assuming the absence of frictional effects and with no arcing occurring ahead of the projectile) will no longer be fully described by equation (1). The equation of motion for the arc-projectile system involving a time-varying L' becomes (see Appendix A):

$$(m_a + m_p) \frac{dv}{dt} = \frac{1}{2} L'(t) I(t)^2 + \frac{1}{2} \frac{I(t)^2 \ell(t)}{v} \frac{d}{dt} L'(t) \qquad (26)$$

where m_a and m_p represent the masses of the arc and projectile respectively and v is the assumed common velocity of the arc-projectile system. The displacement of the projectile is given by $\ell = \ell(t)$ in the above equation. Equation (26) also assumes that the plasma mass m_a is constant, even though in practice it might be expected that m_a is time-dependent.

Since L'(t) decreases with time (see equations (19) and (20)) then the extra term appearing in equation (26) is negative. Hence the accelerating force on the arc-projectile system is continually decreasing even for a constant value of I.

The extra term appearing in equation (26) means that an effective rail inductance per unit length can be re-defined as:

$$L'_{new}(t) = L'(t) + \frac{\ell}{v} \dot{L}'(t) \qquad (27)$$

The accelerating force on the arc-projectile system can now be described by equation (1) except that $L'_{new}(t)$ replaces L'(t).

The uniform current diffusion model can be used to see if the additional term appearing in equation (27) is significant compared with L'(t). After substituting equation (2) into equation (20) and dividing by ℓ the derivative with respect to time of the resulting expression becomes:

$$\dot{L}'(t) = -\frac{1}{2h} \left(\frac{\mu_o}{\pi^3 \sigma t} \right)^{1/2} \operatorname{artan} \left(\frac{2d}{h} \right) \qquad (28)$$

At t = 0 there is a divergence associated with equation (28) but once it is realised that for small times $\ell/v \sim 0(t)$ then the additional term appearing in equation (27) becomes zero at t = 0. Therefore, the additional term in equation (27) is expected to become significant for increasing times.

As mentioned previously a typical firing in the RPIP series took approximately 1 ms. Using this value along with the conductivity (σ) of copper/cadmium set equal to 4.0×10^7 $(\Omega m)^{-1}$ and d/h = 0.65, equation (28) yields a value of about -3.7×10^{-5} H/m-sec for $\dot{L}'(t)$. In addition the

20

projectile displacement ℓ is approximately 0.5 m (the length of the barrel) and v (the exit velocity) is approximately 1 km/s. Therefore,

$$\frac{\ell}{v} \dot{L}'(t) \sim - 1.9 \times 10^{-8} \text{ H/m} \qquad (29)$$

which shows that the extra term appearing in equation (27) is an order of magnitude smaller than $L'(t)$. This term will become significant only if the magnitude of $\dot{L}'(t)$ is much greater than that given by the uniform current diffusion model used to derive equation (28). It will also become significant if the ratio ℓ/v becomes large, which can occur using longer rails or by achieving lower exit velocities.

A better knowledge of how L' decreases with time can be obtained by running the Kerrisk current diffusion program for different times during the acceleration of the arc-projectile system. The predicted current distributions in the rails for each of these times can then be used to evaluate L' after being introduced into the version of equation (25) applicable to rectangular elements in a grid. A plot of L' against time would then reveal a more realistic decrease in L' during acceleration and the gradient of the resulting curve would be $\dot{L}'$. Such a study would indicate just how serious the problem of current diffusion in the rails is.

8. DISCUSSION AND CONCLUSION

In this study some analytic expressions for the rail inductance per unit length have been derived using some simple and idealized current distributions. Among other assumptions, the effect of uncoupled flux has been neglected so that the distinction between the external inductance and internal inductance does not arise. It has been shown that for the cases where the current is distributed in thin sheets, and also where it is distributed uniformly over the entire rail cross-section, the increase in L' becomes quite small when the rail separation-to-rail-height ratio (d/h) exceeds 10. This suggests that a suitable d/h ratio for a railgun is about 10, which is much larger than that of the MRL railgun. However, it is possible that the use of higher d/h ratios could result in plasma-armature instabilities and this would require investigation. The techniques for such analysis, though under consideration, do not yet seem to be adequately developed.

It has also been shown for the MRL railgun, where d/h is equal to 0.65 that the value of L', assuming that the current is uniformly distributed over the entire rail cross-section, is about 60% of the L' value which is obtained assuming the current is in the form of thin sheets on the inner surfaces of the rails. Thus current diffusion into the rails has the potential to affect the performance of a railgun quite substantially.

The rail inductance per unit length has been calculated numerically by Kerrisk in the high-frequency limit. For d/h equal to 0.65, the value of

L' predicted by his code is approximately 0.34 µH/m. This corresponds to an effective skin-depth $\bar{\delta}$ of about 10 mm or about 80% of the entire rail width using equation (19). A value of 0.34 µH/m represents about a 35% reduction in L' compared with the value obtained using the current sheet approach. Therefore the current diffusion has an important influence on railgun performance.

Whilst current diffusion in the rails might be a serious problem there are ways of minimising its effect. For instance if the rail height and thickness of the rails could be kept to a minimum, then L' would not have an opportunity to decrease substantially in the course of a firing. However, this may not be possible because rail damage might increase due to higher stress.

Another method for reducing the effect of current diffusion is to reduce the skin-depth. From equation (2) it can be seen that if the conductivity and/or the magnetic permeability are increased, then the skin depth decreases. Also, if the duration of a firing can be kept to a minimum by reducing the effect of friction on the projectile, the skin-depth will decrease.

When equation (2) is introduced into equation (19) it has been shown that towards the end of a firing L' could have decreased by as much as 13%. This figure has been determined assuming the current diffuses uniformly to an effective and constant skin-depth δ. A more realistic picture of the effect of current diffusion on L' could, perhaps, be obtained by running the Kerrisk CINDA current diffusion program.

9. ACKNOWLEDGEMENT

22

10. REFERENCES

1. Brooks, A.L., Hawke, R.S., Scudder, J.K. and Wozynski, C.D. "Design and Fabrication of Large- and Small-Bore Railguns", IEEE Transactions on Magnetics, Vol. MAG-18, No. 1, 1982.

2. Stainsby, D.F. and Bedford, A.J. "Some Diagnostic Interpretations from Railgun Plasma Profile Experiments", IEEE Transactions on Magnetics, Vol. MAG-20, No. 2, 1984.

3. Kerrisk, J.F. "Current Diffusion in Rail-Gun Conductors", LA-9401-MS, 1982, LANL, New Mexico, USA.

4. Knoepfel, H. "Pulsed High Magnetic Fields", (North-Holland Publishing Co., Amsterdam, 1970).

5. Attwood, S.S. "Electric and Magnetic Fields", (Wiley & Sons, N.Y., 2nd Ed., 1941).

6. Kerrisk, J.F. "Current Distribution and Inductance Calculations for Rail-Gun Conductors", LA-9092-MS, 1981, LANL, New Mexico, USA.

7. Deadrick, F.J., Hawke, R.S. and Scudder, J.K. "MAGRAC - A Railgun Simulation Program", UCRL-84877 Preprint, 1980, LLNL, Ca., USA.

8. Sadedin, D.R. "Efficiency Equations of the Railgun", IEEE Transactions on Magnetics, Vol. MAG-20, No. 2, 1984.

9. Thio, Y.C. "PARA: A Computer Simulation Code for Plasma Driven Electromagnetic Launchers", MRL-R-873, MRL, Maribyrnong, Australia.

10. Batteh, J.H. "Arc-Dynamic Calculations in the Rail Gun", SAI-83/1046, 1983, Science Applications Inc., Georgia, USA.

11. Marshall, R.A. "Plasma Puffing from a Railgun Armature", IEEE Transactions on Magnetics, Vol. MAG-20, No. 2, 1984.

12. Author's analysis to be published as an MRL Report.

13. Kowalenko, V. "Analysis of the Rapid Plasma Intensity Profiles (RPIP) Series of Experiments", MRL Report currently in preparation.

14. Powell, J.D. and Batteh, J.H. "Atmospheric Effects on Projectile Acceleration in the Rail Gun", J. Appl. Phys., Vol. 54, No. 12, 1983.

APPENDIX A

PROJECTILE EQUATION OF MOTION FOR A RAILGUN

In this Appendix the railgun equation-of-motion for the arc-projectile system is derived for a time-dependent rail inductance per unit length parameter L'.

The railgun can be represented by the equivalent circuit in figure 6. Here the power supply consists of a capacitor bank C which is connected in series with a storage inductor L_o via a switch S_1. The capacitor bank is also equipped with a crow-bar switch S_2 and the rails are connected in series with the inductor.

Provided there is no arcing ahead of the projectile, the Kirchoff equation for the circuit in figure 6 can be written (with switches S_1 closed and S_2 open) as:

$$\frac{Q}{C} + \frac{d}{dt}\left(L_o I(t) + \phi\right) + I(t)\left(R(t) + R'(t)\ell(t)\right) + V_o(t) = 0 \qquad \text{(A-1)}$$

In the above equation, Q represents the instantaneous charge on the capacitor bank, ϕ represents the magnetic flux produced by the current in the rails, R(t) represents the sum of the resistances in the circuit such as the resistances of the switches and busbars while R'(t) represents the effective time-dependent resistance per unit length of the rails. $V_o(t)$ represents any time-varying extraneous potential that may exist within the circuit. The displacement of the projectile is denoted by ℓ as depicted in figure 1.

If equation (A-1) is multiplied by the current I in the circuit and then integrated over time t from t=0 to $t=t_1$, then equation (A-1) becomes:

$$\int_o^{t_1} \frac{IQ}{C}\, dt + \int_o^{t_1} I\frac{d}{dt}\left(L_o I(t) + \phi\right)dt + \int_o^{t_1} I^2\left(R(t) + R'(t)\ell\right)dt$$

$$+ \int_o^{t_1} I\, V_o(t)\, dt = 0 \qquad \text{(A-2)}$$

where I(0) = 0. Equation (A-2) can be re-cast in the following form

$$E(0) = \frac{Q^2(0)}{2C} = \frac{Q^2(t_1)}{2C} + \frac{1}{2}L_o I^2(t_1) + \int_o^{t_1} I\frac{d}{dt}\phi\, dt$$

$$+ \int_o^{t_1} I^2(t)\left(R(t) + R'(t)\ell(t)\right)dt + \int_o^{t_1} I(t)\, V_o(t)dt \qquad \text{(A-3)}$$

where E(0) is the total initial energy.

Now by definition the magnetic flux ϕ between the rails is:

$$\phi = LI(t) \tag{A-4}$$

where L represents the inductance of the rails. After substituting equation (A-4) into equation (A-2) the following equation is obtained:

$$E(0) = \frac{Q^2(t_1)}{2C} + \frac{1}{2} L_o I^2(t_1) + \frac{1}{2} (I\phi) \Big|_{t=0}^{t_1} + \int_o^{t_1} I^2(t)\big(R(t) + R'(t)\ell(t)\big)dt$$

$$+ \int_o^{t_1} I(t) V_o(t) dt + \frac{1}{2} \int_o^{t_1} I^2 dL \tag{A-5}$$

The first three terms in equation (A-5) represent the energies stored by the capacitor bank, the storage inductor and the rails at time t_1. The next two terms represent the energies dissipated by the resistances in the circuit and the extraneous potential. The final expression in equation (A-5) must clearly account for other energy distribution in the system including that related to the motion of the arc-projectile system and therefore must account for (1) the kinetic energy of the projectile, (2) the kinetic energy of the plasma material, (3) the work done on the gas in front of the projectile, (4) the work done on overcoming frictional forces on the projectile, and (5) the work done on overcoming the frictional or drag forces on the plasma-armature.

The kinetic energy of the projectile is:

$$E_1 = \frac{1}{2} m_p v^2(t_1) \tag{A-6}$$

where m_p is the assumed constant mass of the projectile. On the other hand the kinetic energy of the plasma armature is:

$$E_2 = \frac{1}{2} \sum_i N_i m_i v_i^2 \tag{A-7}$$

which is a summation over all species with mass m_i and average velocity v_i. It is customary to represent equation (A-7) by the term $m_a v^2/2$ where m_a is the so-called armature mass, which is assumed constant. The major assumption here is that this armature mass is assumed to be travelling at the same velocity as the projectile.

The retarding forces on the projectile due to gas ahead of it has been discussed by Powell and Batteh [14] in terms of a shock pressure $P_s(t)$, which is a function of projectile velocity $v(t)$. If this approach is valid then the related energy term will be of the form:

$$E_3 = A_p \int_o^{t_1} P_s(t) v(t) dt \tag{A-8}$$

where A_p is the bore (and projectile) cross-sectional area.

The work done on overcoming the frictional forces on the projectile will be of the form:

$$E_4 = \int_o^{t_1} f_p(t) \, v(t) \, dt \qquad (A-9)$$

Unfortunately very little is known about the nature of $f_p(t)$.

A similar expression (and lack of knowledge) applies to frictional drag on the plasma armature. If the plasma is composed of a fixed set of ions then the frictional effect could be low. If, however, there is a movement of material into and out of the plasma from the rails then additional drag forces which could be described as frictional forces will operate. The work to overcome this drag will be described by:

$$E_5 = \int_o^{t_1} f_a(t) v(t) \, dt \qquad (A-10)$$

where, at this stage, the form and nature of $f_a(t)$ is unknown.

After the energy terms described by equations (A-6) through to (A-10) are summed, and if it is assumed that other possible energy-dissipation mechanisms are negligible, then the sum can be equated to the final expression of equation (A-5), giving the following equation:

$$\frac{1}{2} \int_{t=0}^{t_1} I(t)^2 \, dL = \frac{1}{2} v^2(t_1) \, (m_p + m_a) + \int_o^{t_1} v(t) \left(f_a(t) + f_p(t) \right) dt$$

$$+ A_p \int_o^{t_1} P_s(t) \, v(t) \, dt \qquad (A-11)$$

For the sake of generality and also to be consistent with the model assumed in this paper, the inductance of the rails is considered to be a function of the projectile's displacement, ℓ and the time, t. Equation (A-11) then becomes:

$$\frac{1}{2} \int_{t=0}^{t_1} I(t)^2 \left(\frac{\partial L}{\partial \ell} \, d\ell + \frac{\partial L}{\partial t} \, dt \right) = \frac{1}{2} v^2(t_1)(m_p + m_a) + \int_0^{t_1} v(t) \left(f_a(t) + f_p(t) \right) dt$$

$$+ A_p \int_0^{t_1} P_s(t) \, v(t) \, dt \qquad (A-12)$$

After differentiation of equation (A-12) with respect to time t_1 the following equation is obtained:

$$(m_a + m_p) \frac{dv}{dt} = \frac{1}{2} \frac{\partial L}{\partial \ell} I(t)^2 + \frac{1}{2} \frac{I(t)^2}{v} \frac{\partial L}{\partial t} - f(t) \qquad \text{(A-13)}$$

where f(t) is a general term involving the drag and frictional forces on the arc-projectile system and t has now replaced t_1 as the general time variable.

Throughout this report the inductance of the rails has been taken to be of the following form:

$$L = L'(t)\ell \qquad \text{(A-14)}$$

where L'(t) is defined as the average inductance per unit length of the rails and is time-dependent. Once equation (A-14) is introduced into equation (A-14) the following equation appears:

$$(m_a + m_p) \frac{dv}{dt} = \frac{1}{2} L'(t) I(t)^2 + \frac{1}{2} \frac{\ell}{v} I(t)^2 \frac{dL'(t)}{dt} - f(t) \qquad \text{(A-15)}$$

If L'(t) is a constant given by L', then equation (A-15) simplifies to:

$$(m_a + m_p) \frac{dv}{dt} = \frac{1}{2} L' I(t)^2 - f(t) \qquad \text{(A-16)}$$

If further, f(t) = 0, then it follows that the effective accelerating force F(t) is given by:

$$F(t) = \frac{1}{2} L' I(t)^2 \qquad \text{(A-17)}$$

It is noted that equations (A-13), (A-15), (A-16) and (A-17) are independent of the electrical network parameters external to the rail projectile system itself and thus the equations could have been obtained without directly defining the nature of the 'external' power circuit. Although the actual current I(t) will depend on the entire railgun circuit, equations (A-13), (A-15) and (A-16) are quite general and apply to both pre- and post-crowbarring of the capacitor bank. It is stressed that the inductance of the rails is the sum of two quantities, one being the external inductance, which has been determined throughout this report and the other being the internal inductance, which has been considered to be negligible.

APPENDIX B

THE HAWKE-SADEDIN MODEL FOR CURRENT DIFFUSION

In this Appendix the possibility of using the more realistic and interesting Hawke-Sadedin model for current diffusion or penetration into the rail is considered in a calculation of the rail inductance per unit length.

The model for current diffusion used by Hawke and Sadedin is depicted in figure 7. Here it is shown that at a distance s from the breech end of a railgun the current has penetrated a depth δ. The difference between this model and the effective skin-depth model proposed earlier is that the skin-depth is now dependent upon the time variable $t-t_s$, where t_s is the time taken for the projectile to reach s and t is the time the projectile has travelled. Thus this model incorporates the notion of causality where diffusion of current occurs only when t is greater than each t_s, i.e. when the projectile has passed each position s along the barrel.

Before the rail inductance can be evaluated, the magnetic field of induction at the point P with co-ordinates $(x',y',0)$ between the rails as indicated in figure 1 must be found. In using the Hawke-Sadedin model it is best to consider an alternative form of the Biot-Savart law (i.e. equation (3)). Therefore the total magnetic field is given by:

$$\underline{B} = \int d\underline{B} = \int \frac{\mu_o \underline{j} \times \underline{r}}{4\pi r^3} \, dV \tag{B-1}$$

where $\underline{r}$ is once again the position vector from the current element to the point P and dV is the volume element, which becomes at s::

$$dV = dz \, dx \, v(t_s) \, dt_s \tag{B-2}$$

In equation (B-1) $\underline{j}$ represents the current density and in equation (B-2) $v(t_s)$ represents the velocity of the projectile at s.

Although the penetration depth δ varies with time, the current in this model is assumed to diffuse uniformly to that depth δ. Thus the magnitude of the current density at the position s becomes:

$$j = \left|\underline{j}\right| = \frac{I(t)}{h\delta(t-t_s)} H(t-t_s) \tag{B-3}$$

where $\delta(t-t_s)$ is the skin-depth given by equation (2), h is the height of the rails, $I(t)$ is the current in the circuit and $H(x)$ is the Heaviside step-function, which is defined as:

$$H(x) = \begin{cases} 1 & x > 0 \\ 0 & x < 0 \end{cases} \tag{B-4}$$

After application of equation (B-1), the total magnetic field at the point P due to the left rail is:

$$B = \int_0^t \int \delta(t-t_s) \int_{-h/2}^{h/2} \frac{\mu_0}{4\pi} \frac{I(t) \, H(t-t_s)}{h\delta(t-t_s)} \, \hat{y} \times \frac{((x'-x)\hat{x} + (y'-y(t_s))\hat{y} - z\,\hat{z})}{((x'-x)^2 + (y'-y(t_s))^2 + z^2)^{3/2}} \times$$

$$v(t_s) \, dz dx dt_s \tag{B-5}$$

The order of integration between the dx and dt_s integrals is now important whereas when using the effective skin-depth model the order was of no consequence. It should be noted that the dt_s-integral has replaced the dy-integral and that the length y must become a function of t_s.

The z-component of the magnetic field of induction is the component which contributes to the propelling magnetic flux. This is:

$$B_z = -\int_0^t \int \delta(t-t_s) \int_{-h/2}^{h/2} \frac{\mu_0}{4\pi} \frac{I(t)H(t-t_s)}{h\delta(t-t_s)} \frac{(x'-x)v(t_s)\,\hat{z}\, dx\, dx\, dt_s}{((x'-x)^2 + (y'-y(t_s))^2 + x^2)^{3/2}} \tag{B-6}$$

The dx-integral is identical to that in equation (6) and hence after integration equation (B-6) becomes:

$$B_z = \int_0^t v(t_s) \int_0^{h/2} \frac{\mu_0}{2\pi} \frac{I(t) \, H(t-t_s)}{h\delta(t-t_s)} \hat{z} \left(\frac{1}{((y'-y(t_s))^2 + x'^2 + z^2)^{1/2}} \right.$$

$$\left. - \frac{1}{((y'-y(t_s))^2 + (x'-\delta(t-t_s))^2 + z^2)^{1/2}} \right) dz \, dt_s \tag{B-7}$$

After performing the dz-integral, equation (B-7) takes the following form:

$$B_z = \int_0^t \frac{v(t_s) \, \mu_0 \, \hat{z}}{2\pi} \frac{I(t)H(t-t_s)}{h\delta(t-t_s)} \left(\ln \left| \frac{h/2 + ((y'-y(t_s)^2 + x'^2 + h^2/4)^{1/2}}{h/2 + ((y'-y(t_s))^2 + (x'-\delta(t-t_s))^2 + h^2/4)^{1/2}} \right| \right.$$

$$\left. - \tfrac{1}{2}\ln \left| \frac{(y'-y(t_s))^2 + x'^2}{(y'-y(t_s))^2 + (x' - \delta(t-t_s))^2} \right| \right) dt_s \tag{B-8}$$

Therefore before the z-component of the magnetic field and hence the rail inductance can be found, a knowledge of $v(t_s)$ and $y(t_s)$ is required. The velocity $v(t_s)$ and displacement $y(t_s)$ are obtained by solving the railgun equation of motion, i.e. equation (A-13). However, before this equation can be solved, a knowledge of the rail inductance per unit length, amongst other physical quantities, is required. Therefore before the rail inductance can be evaluated using the Hawke-Sadedin model, the rail inductance must be known as a function of time. This difficulty indicates that the quasi-stationary approach used in this study cannot be applied to the Hawke-Sadedin model. As a result of this, the simpler uniform effective skin-depth model has been considered.
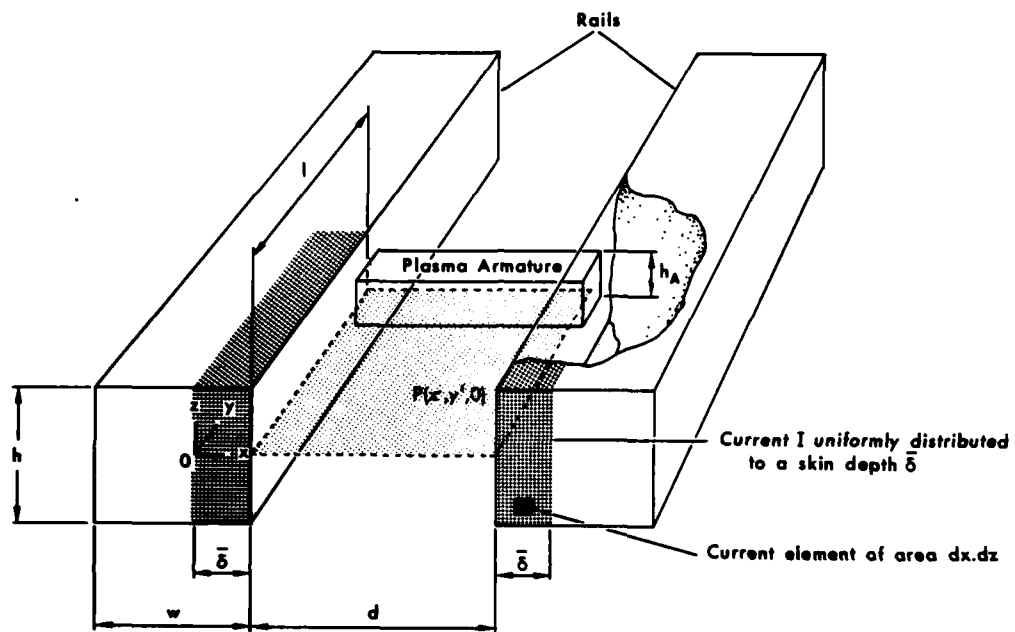
FIGURE 1   The model.
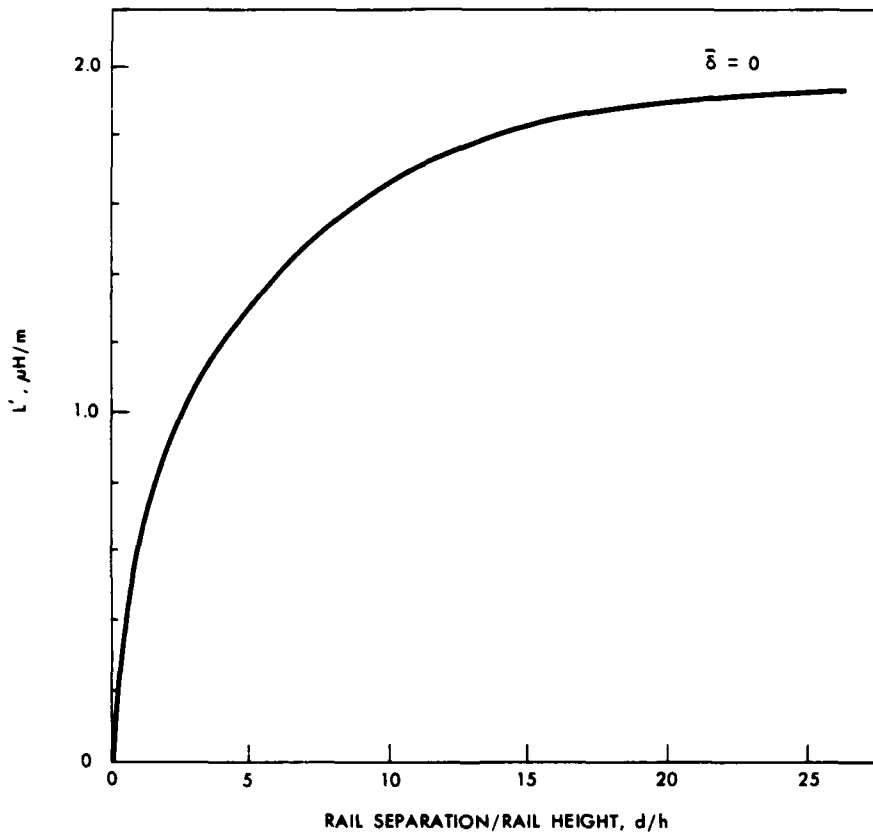
FIGURE 2   Rail inductance per unit length vs. d/h for zero skin depth.
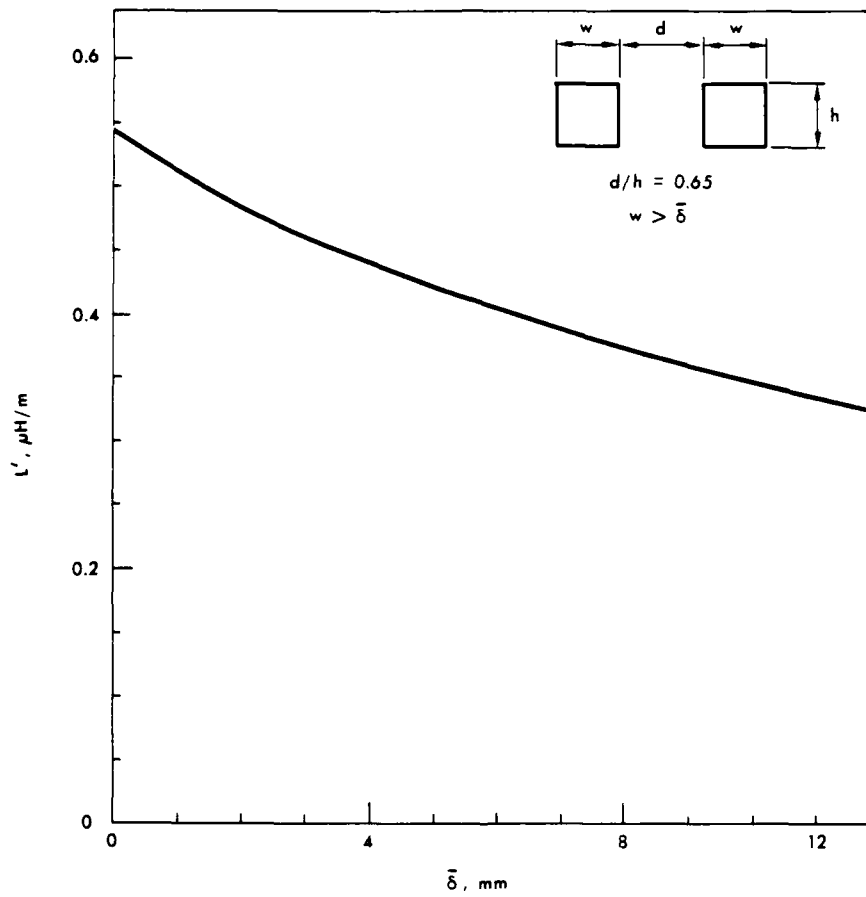
FIGURE 3   Rail inductance per unit lengths vs. effective skin-depth.
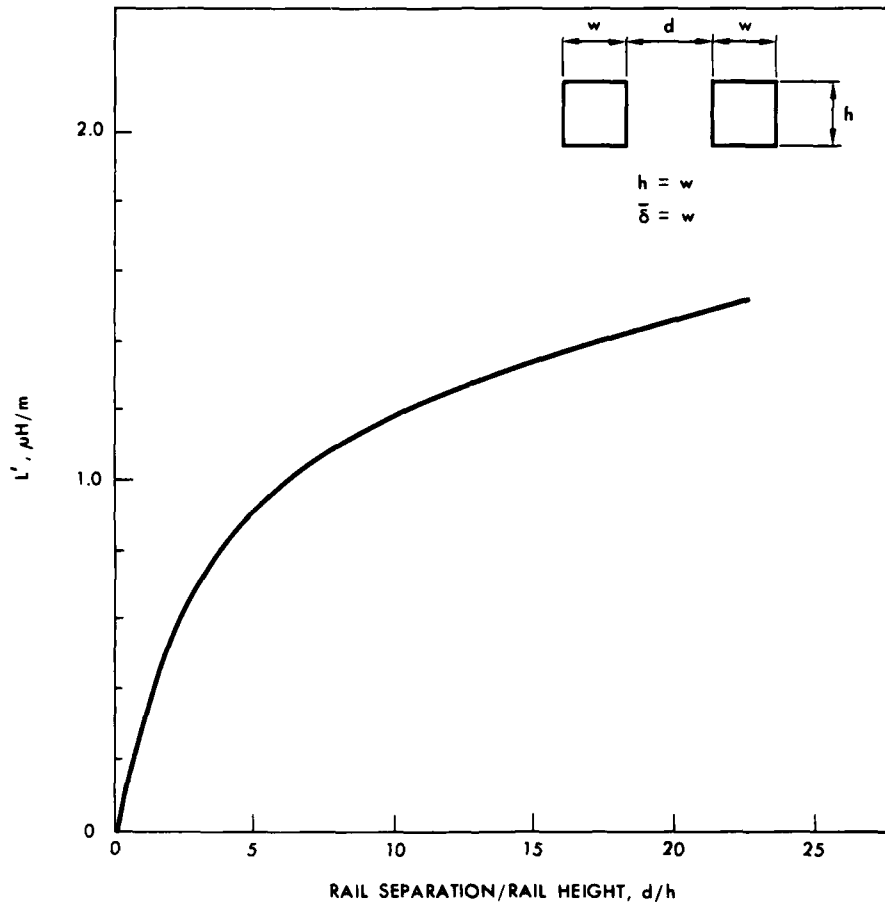
FIGURE 4   L' vs. (d/h) for current uniformly distributed over square rail cross-section.

I_{16}	I_{15}	I_{14}	I_{13}	I_{12}	I_{11}
I_{26}	I_{25}	I_{24}	I_{23}	I_{22}	I_{21}
I_{36}	I_{35}	I_{34}	I_{33}	I_{32}	I_{31}
I_{46}	I_{45}	I_{44}	I_{43}	I_{42}	I_{41}
I_{46}	I_{45}	I_{44}	I_{43}	I_{42}	I_{41}
I_{36}	I_{35}	I_{34}	I_{33}	I_{32}	I_{31}
I_{26}	I_{25}	I_{24}	I_{23}	I_{22}	I_{21}
I_{16}	I_{15}	I_{14}	I_{13}	I_{12}	I_{11}

FIGURE 5   A finite element grid for a rail.   Here n=4 and m=6.
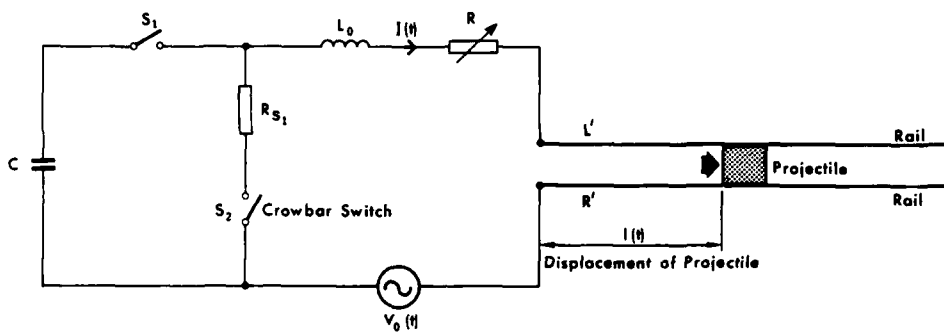
FIGURE 6   Equivalent railgun circuit.
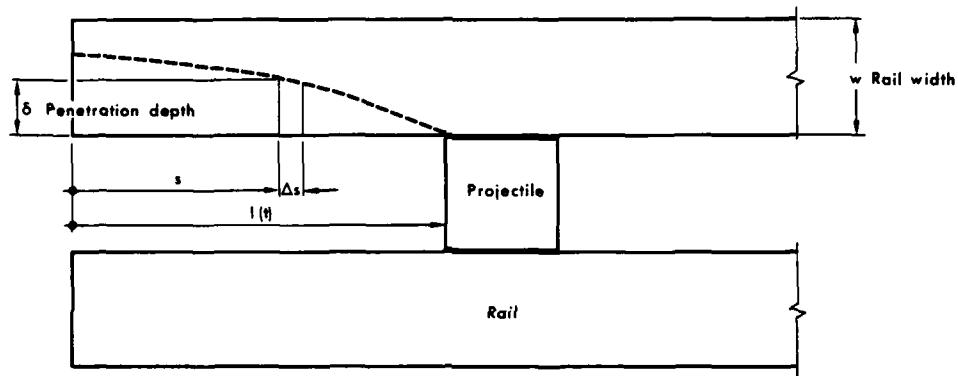
FIGURE 7   The Hawke-Sadedin model for current diffusion into the rails.

END
DTIC
6-86